

Electronic Supplementary Information

Facet-Dependent Oxysulfidation of Cu₂O Nanomaterials: Implications for Improving the Efficacy of Nanopesticides

Tingting Du¹, Wenyu Guan², Zhanhua Zhang², Chuanjia Jiang², Pedro J. J. Alvarez³, Wei Chen²,
Tong Zhang^{2*}

¹ Information Materials and Intelligent Sensing Laboratory of Anhui Province, Institutes of Physical Science and Information Technology, Anhui University, Hefei 230601, China

² College of Environmental Science and Engineering, Ministry of Education Key Laboratory of Pollution Processes and Environmental Criteria, Tianjin Key Laboratory of Environmental Remediation and Pollution Control, Nankai University, Tianjin 300350, China

³ Department of Civil and Environmental Engineering, Rice University, 6100 Main Street, Houston, TX 77005, USA

Number of pages: 12

Number of tables: 3

Number of figures: 6

* Corresponding authors: (E-mail) zhangtong@nankai.edu.cn.

S1. Chemicals.

Cupric chloride dihydrate ($\text{CuCl}_2 \cdot 2\text{H}_2\text{O}$), cupric sulfate (CuSO_4), polyvinylpyrrolidone (PVP, molecular weight = 30000), sodium hydroxide (NaOH), ascorbic acid, oleic acid, D-(+)-glucose, sodium sulfide nonahydrate ($\text{Na}_2\text{S} \cdot 9\text{H}_2\text{O}$), 4-hydroxyethylpiperazine-1-propanesulfonic acid (HEPPS), and 2,9-dimethyl-1,10-phenanthroline (neocuproine) were purchased from Aladdin Co. Ltd. Ethanol and cyclohexane were obtained from Tianjin Chemical Reagent Co. All chemicals were analytical grade and used without further purification. Deionized (DI) water was used in all experiments.

S2. Oxidation of Cu_2O nanomaterials.

The oxidation of Cu_2O nanomaterials with different exposed facets was investigated in batch tests. High-purity O_2 was purged into 20 mL of aqueous solution containing 50 mg of Cu_2O nanomaterials. After 9 h of reaction, the oxidized Cu_2O nanomaterials were collected by centrifugation at 13000 g for 15 min and allowed to dry in a vacuum-freezing dryer to obtain the solid materials for characterization by X-ray diffraction (XRD).

Table S1 Selected physicochemical properties of Cu₂O nanomaterials.

Samples	Shape	d^a (nm)	Predominant exposed facet
Cu ₂ O_{100}	cube	887 ± 135	{100}
Cu ₂ O_{111}	octahedron	860 ± 97	{111}
Cu ₂ O_{110}	rhombic dodecahedron	509 ± 80	{110}

^a d = edge length of single nanomaterials determined by counting 200 particles in SEM images.

Table S2 Sulfur to copper (S/Cu) ratio of oxysulfidized Cu₂O nanomaterials at reaction time of 1 day.

Samples	Atomic ratio of S/Cu ^a
Oxysulfidized Cu ₂ O_{100}	0.98
Oxysulfidized Cu ₂ O_{111}	0.96
Oxysulfidized Cu ₂ O_{110}	0.67

^a Analyzed by energy dispersive X-ray spectroscopy (EDS) attached to the SEM.

Table S3 Crystalline phases identified in oxysulfidized Cu₂O nanomaterials at different reaction times.

Samples	Crystalline phases ^a (10 min)	Crystalline phases ^a (1 day)
Oxysulfidized Cu ₂ O_{100}	cuprite@yarrowite-covellite	covellite
Oxysulfidized Cu ₂ O_{111}	cuprite@yarrowite	covellite
Oxysulfidized Cu ₂ O_{110}	cuprite@djurleite	cuprite@covellite

^a Analyzed by X-ray diffraction (XRD) and determined using MDI Jade 6 software, where cuprite corresponds to Cu₂O (JCPDS No. 05-0667), djurleite corresponds to Cu₃S₁₆ (JCPDS No. 34-0660), yarrowite corresponds to Cu₉S₈ (JCPDS No. 36-0379), and covellite corresponds to CuS (JCPDS No. 06-0464).

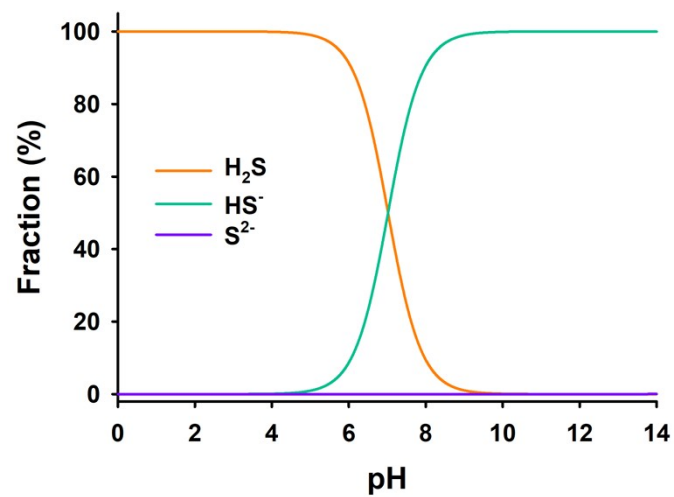


Fig. S1 Mass fractions of different sulfide species (H_2S , HS^- , and S^{2-}) in aqueous solution as a function of pH at 25 °C. Calculations are based on $\text{p}K_{\text{a}1} = 7.02$, $\text{p}K_{\text{a}2} = 17.4$.¹

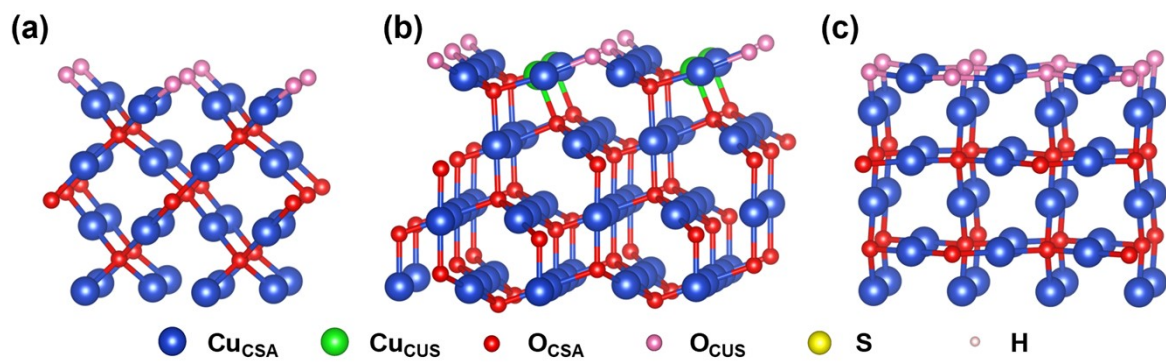


Fig. S2 Side views of optimized geometric structures (a-c) of Cu_2O nanomaterials: $\text{Cu}_2\text{O}_{\{100\}}$ (a); $\text{Cu}_2\text{O}_{\{111\}}$ (b); and $\text{Cu}_2\text{O}_{\{110\}}$ (c).

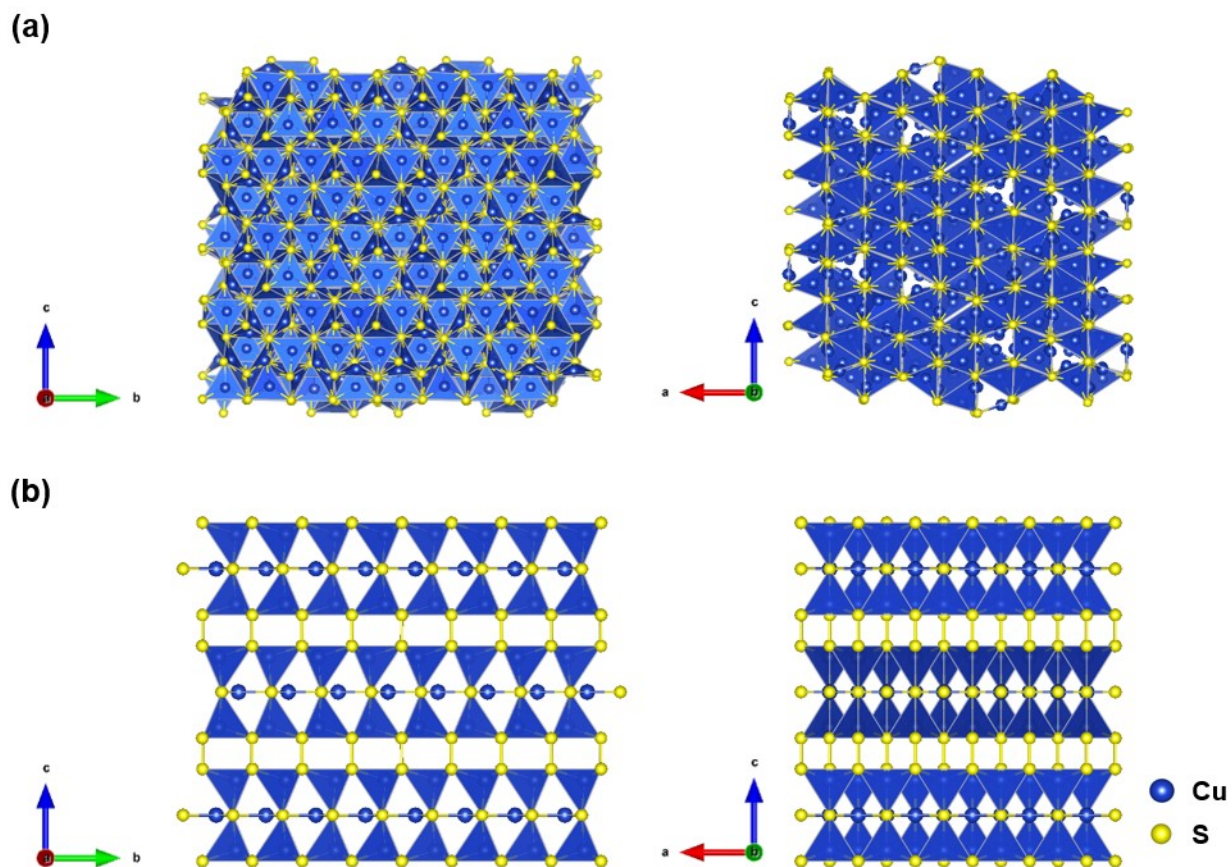


Fig. S3 Crystal structure of djurleite (a) and covellite (b) (data from American Mineral Crystal Structure Database, <http://ruff.geo.arizona.edu/AMS/amcsd.php>). The crystal structure of yarrowite is not displayed as it is still not determined.²

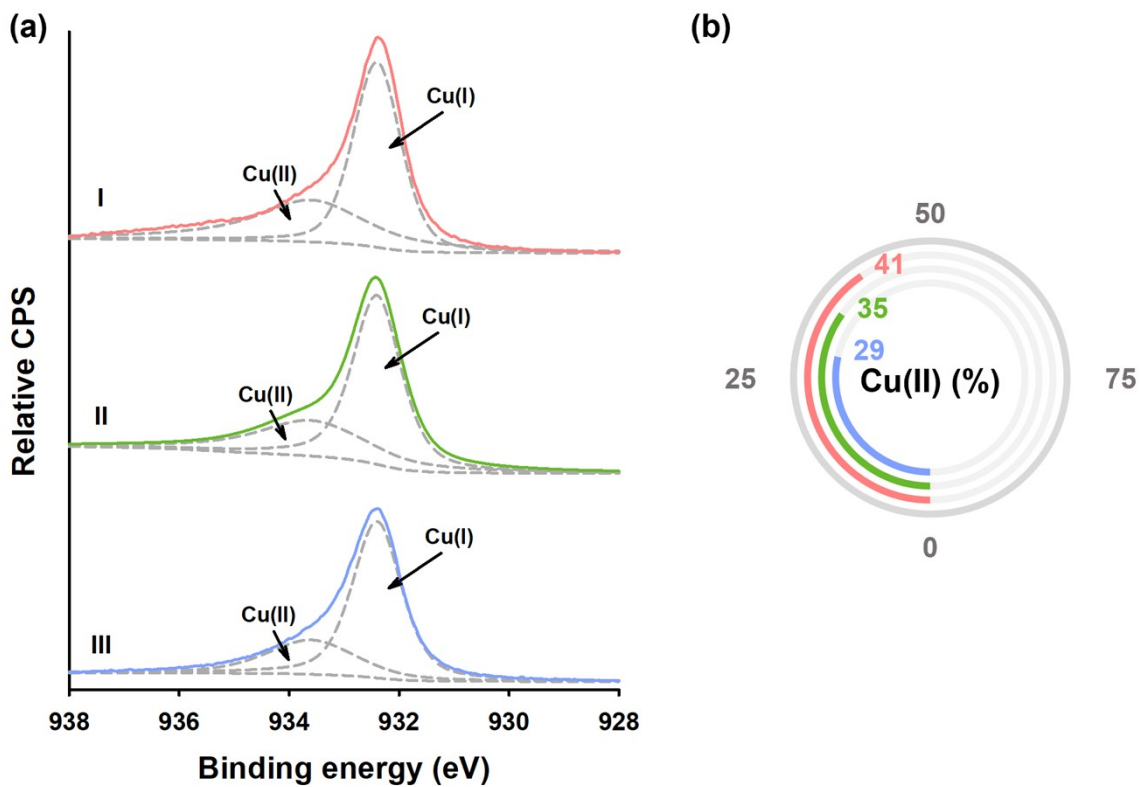


Fig. S4 Deconvoluted Cu 2p X-ray photoelectron spectroscopy (XPS) spectra (a) and the proportion of Cu(II) (b) of initial oxysulfidation products of Cu_2O nanomaterials after 10 min of reaction (I: oxysulfidized $\text{Cu}_2\text{O}_{\{100\}}$; II: oxysulfidized $\text{Cu}_2\text{O}_{\{111\}}$; III: oxysulfidized $\text{Cu}_2\text{O}_{\{110\}}$; these initial oxysulfidation products are represented by red, green, and blue colors in part b).

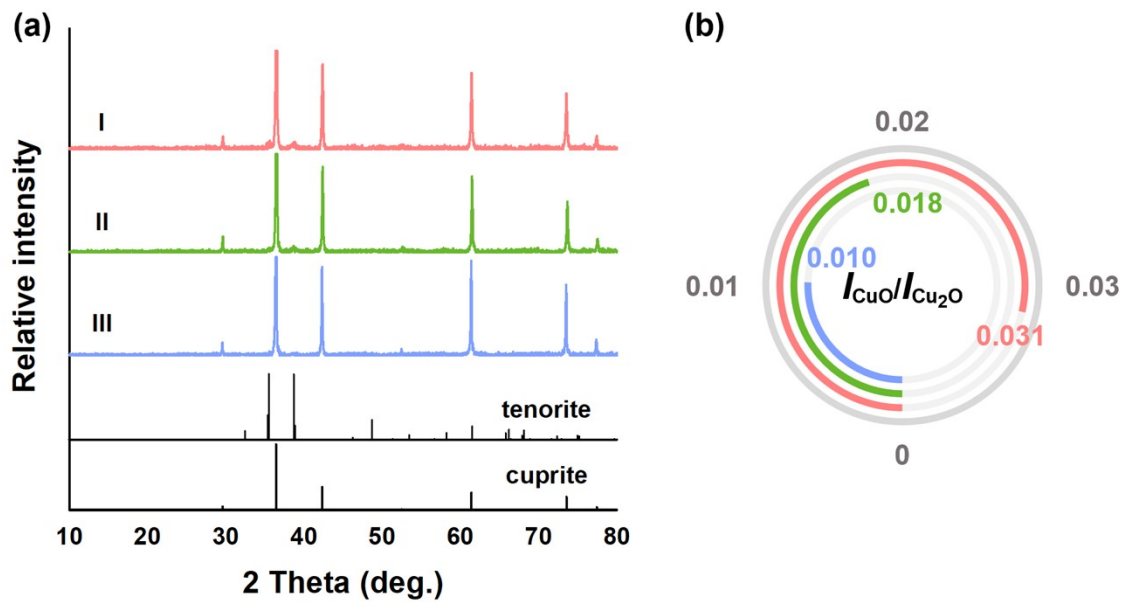


Fig. S5 XRD patterns of oxidized Cu₂O nanomaterials (a) and the ratio of the intensity of the highest peak of the CuO phase to that of the Cu₂O phase (b) (I: oxidized Cu₂O_{100}; II: oxidized Cu₂O_{111}; III: oxidized Cu₂O_{110}; these oxidized products are represented by red, green, and blue colors in part b).

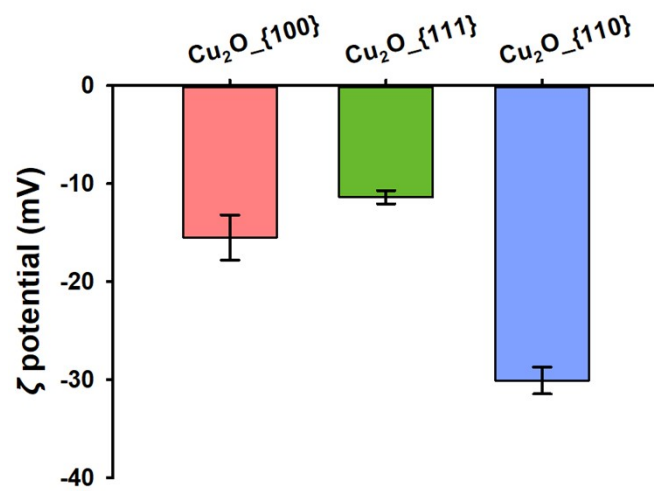


Fig. S6 ζ potential of Cu₂O nanomaterials in HEPPS buffer.

References

1. M. M. Benjamin, *Water Chemistry*, Waveland Press, Inc., 2014.
2. P. Roy and S. K. Srivastava, Nanostructured copper sulfides: Synthesis, properties and applications, *CrystEngComm*, 2015, **17**, 7801–7815.